

引用格式: ZHANG Zihao, HU Haowen, LIAO Junyi, et al. Passively Q-switched and Mode-locked All-fiber Yb-doped Laser with  $\beta$ -InSe Saturable Absorber (Invited)[J]. Acta Photonica Sinica, 2021, 50(10):1014003  
张子灏, 胡皓闻, 廖俊懿, 等. 基于  $\beta$  相硒化铟的被动调 Q 及锁模掺镱光纤激光器(特邀)[J]. 光子学报, 2021, 50(10):1014003

## 基于 $\beta$ 相硒化铟的被动调 Q 及锁模掺镱光纤 激光器(特邀)

张子灏<sup>1</sup>, 胡皓闻<sup>2</sup>, 廖俊懿<sup>3</sup>, 朱宏伟<sup>2</sup>, 谢黎明<sup>3,4</sup>, 王军利<sup>1</sup>, 魏志义<sup>5</sup>

(1 西安电子科技大学 物理与光电工程学院, 西安 710071)

(2 清华大学 材料科学与工程学院, 北京 100084)

(3 国家纳米科学中心 中国科学院纳米标准与检测重点实验室, 北京 100190)

(4 中国科学院大学, 北京 100049)

(5 中国科学院物理研究所 北京凝聚态物理国家实验室, 西安 100190)

**摘要:** 利用层状半导体  $\beta$  相硒化铟作为可饱和吸收体, 在掺镱光纤激光器中实现稳定的调 Q 及锁模运转。经测量该可饱和吸收体在 1  $\mu\text{m}$  波段调制深度及非饱和损耗分别为 47% 及 20%。将可饱和吸收体插入掺镱光纤激光器中, 可获得 53.42 kHz 到 217 kHz 重频可调的调 Q 脉冲。其最窄脉冲宽度为 630 ns, 最大单脉冲能量为 47.9 nJ。优化激光谐振腔后可进一步实现稳定的锁模输出, 其重频为 10.82 MHz, 最大输出功率为 51.2 mW, 最大单脉冲能量为 4.7 nJ。实验证明了  $\beta$  相硒化铟作为可饱和吸收体在近红外超快非线性光学方面的潜力。

**关键词:** 可饱和吸收体; 调 Q 激光; 光纤激光器; 锁模激光; 硒化铟

中图分类号: TN248; TN304.2

文献标识码: A

doi:10.3788/gzxb20215010.1014003

## Passively Q-switched and Mode-locked All-fiber Yb-doped Laser with $\beta$ -InSe Saturable Absorber (Invited)

ZHANG Zihao<sup>1</sup>, HU Haowen<sup>2</sup>, LIAO Junyi<sup>3</sup>, ZHU Hongwei<sup>2</sup>, XIE Liming<sup>3,4</sup>,  
WANG Junli<sup>1</sup>, WEI Zhiyi<sup>5</sup>

(1 School of Physics and Optoelectronic Engineering, Xidian University, Xi'an 710071, China)

(2 School of Materials Science and Engineering, Tsinghua University, Beijing 100084, China)

(3 CAS Key Laboratory of Standardization and Measurement for Nanotechnology, National Center for Nanoscience and Technology, Chinese Academy of Sciences, Beijing 100190, China)

(4 University of Chinese Academy of Sciences, Beijing 100049, China)

(5 Beijing National Laboratory for Condensed Matter Physics, Institute of Physics, Chinese Academy of Sciences, Beijing 100190, China)

**Abstract:** A stable Q-switched and mode-locked Ytterbium Doped Fiber Laser (YDFL) based on layered semiconductor  $\beta$ -InSe as Saturable Absorber (SA) were demonstrated for the first time. The modulation depth and non-saturable absorbance of the SA were 47% and 20%, respectively. After inserting the SA

**Foundation item:** National Key Research and Development Program of China (No. 2018YFB1107200)

**First author:** ZHANG Zihao (1997—), male, lecturer, Ph.D candidate, mainly focuses on fiber amplifier technology and application. Email: zhzhang311@stu.xidian.edu.cn

**Supervisor (Contact author):** WANG Junli (1976—), male, professor, Ph.D. degree, mainly focuses on advanced fiber laser and laser micro/nano-fabrication. Email: dispersion@126.com

**Received:** Jul.20, 2021; **Accepted:** Aug.30, 2021

http://www.photon.ac.cn

into YDFL, the stable Q-switched pulse operation can be easily obtained with the repetition rate range from 53.42 kHz to 217 kHz. The minimum pulse duration was 630 ns and the maximum single pulse energy was 47.9 nJ. By optimizing the laser resonator, a stable mode-locking pulse with repetition rate of 10.82 MHz, maximum output power of 51.2 mW and maximum single pulse energy of 4.7 nJ can be achieved. The experimental results demonstrated that  $\beta$ -InSe SA has great potential in near infrared ultrafast nonlinear optical.

**Key words:** Saturable absorbers; Q-switched lasers; Fiber lasers; Mode-locked lasers; Indium selenides

**OCIS Codes:** 140.3510; 140.3540; 140.3615; 140.4050; 160.4330

## 0 Introduction

Compared with Continuous Wave (CW) fiber lasers, pulse fiber lasers have the advantage of narrow pulse duration and high pulse energy. In recent years, it has developed rapidly in many fields, such as optical frequency comb, laser waveguide, optical fiber communication, biomedicine and so on<sup>[1]</sup>. In order to modulate the laser operation from CW into pulsed regime, passive Q-switching and passive mode-locking technology have become the mainstream of the laser development due to their low cost and all-fiber structure. SA is the most critical device for pulse generation. At present, the most stable saturable absorber is Semiconductor Saturable Absorber Mirrors (SESAMs)<sup>[2]</sup>. However, some problems, such as high production cost and low damage threshold that limit the maximum output power, remain to be solved. Therefore, the SAs with high modulation depth, high damage threshold and high stability have attracted more attentions. Two dimensional layered semiconductor materials, a kind of SAs with ultrafast recovery time, wide absorption range and adjustable band gap, mainly divided into three types: Transition-Metal Dichalcogenides (TMDs)<sup>[3-5]</sup>, Black Phosphorus (BPs)<sup>[6-8]</sup>, and III-VI compound layered semiconductors<sup>[9-10]</sup>.

III-VI compound layered semiconductors have great application prospects in infrared detection, photoelectric devices and solar cells due to the characteristics of small band gap and high environmental stability<sup>[9]</sup>. III-VI compound layered semiconductors with a variety of crystal structures and stacking arrangements are mainly divided into MX (such as InSe, GaSe, GaS and GaTe) and  $M_nX_b$  (such as  $In_2Se_3$  and  $In_3Se_4$ ). For example, InSe has four different crystal configurations, which are  $\beta$ ,  $\epsilon$ ,  $\gamma$ ,  $\delta$ <sup>[11]</sup>. The two most common configurations are  $\beta$ -InSe and  $\gamma$ -InSe. InSe and  $In_2Se_3$  have a direct band gap of 1.26 eV and 1.36 eV, respectively. Fiber laser based on  $In_2Se_3$  SA have been widely reported recently. In 2018, YAN Peiguang, et al<sup>[12]</sup> studied the wideband saturable absorption property of  $In_2Se_3$  at 800, 1 560, and 1 930 nm, and by using  $In_2Se_3$  as SA, which a mode-locking operation can be achieved. The same year, AHMAD H, et al<sup>[13]</sup> demonstrated passively Q-switched Bi-EDF laser with an  $In_2Se_3$  SA, the maximum available pump power of 134 mW and a wide tuning range of 40 nm, covering a wavelength range of 1 533 nm to 1 573 nm. In 2020, HAI Ting, et al<sup>[14]</sup> proved  $In_2Se_3$  SA can be used for fiber lasers in the 3 to 4  $\mu$ m waveband. WANG Lizhen, et al<sup>[15]</sup> reported stable mode-locked soliton pulses with 158 fs pulse duration and 2.72 mW average power based on graphene/ $\alpha$ - $In_2Se_3$  heterostructure SA. In 2021, LI Lu, et al<sup>[16]</sup> obtained a dual-wavelength Q-switched EDF laser. The narrowest pulse duration and largest pulse energy was 556 ns and 376 nJ, respectively. However, most report based on  $In_2Se_3$  operate in anomalous dispersion region, and the 1  $\mu$ m fiber laser based on InSe SA had not been studied yet.

In this work, we constructed a YDFL by using  $\beta$ -InSe nonflakes as SA, which was sandwiched into two FC/APC fiber end face with a fiber flange. After inserting the SA into YDFL system, a stable Q-switched pulse with minimum pulse duration of 0.63  $\mu$ s and the maximum pulse energy of 47.9 nJ can be achieved. Meanwhile, A stable mode-locked pulse operation was generated after optimization with the maximum output power of 51.2 mW, corresponding to the maximum pulse energy of 4.7 nJ. Our YDFL system based on  $\beta$ -InSe SA have the advantage of the compact structure, low production cost and independent of the polarization evolution in the cavity. All polarization-maintaining structure can be used to further enhance its stability.

## 1 $\beta$ -InSe SA fabrication and characterization

Bulk InSe was prepared in a tube furnace by the Bridgman method. In addition, InSe nanoflakes were prepared by mechanical exfoliation with 3M Scotch tape.  $\beta$ -InSe, belonging to the  $D_{6h}^4$  space group, consists of

four atomic layers (Se-In-In-Se), and each layer is connected by van der Waals (vdWs) interactions arranged in a hexagonal atomic lattice. The structure and composition of  $\beta$ -InSe were confirmed by Raman spectroscopy, X-Ray Diffraction (XRD), Scanning Electron Microscope (SEM), and Energy Dispersive Spectrometer (EDS). Three prominent peaks at 118, 181, and 230  $\text{cm}^{-1}$  were observed, which correspond to the  $A_{1g}^1$ ,  $E_{2g}^1$ , and  $A_{1g}^2$  vibration modes of  $\beta$ -InSe, respectively (Fig. 1(a)). As shown in Fig. 1(b), typical XRD pattern matches well with the standard data file PDF 34-1431, indexing  $a=b=0.40$  nm and  $c=1.66$  nm of each unit cell. Fig. 2 displays the appearance and the composition of bulky  $\beta$ -InSe crystal. The two elements (In and Se) were uniformly distributed in the material, and the atomic ratio of In/Se was around 1:1. All of those measurements indicate the high crystalline quality of the as-grown  $\beta$ -InSe crystal.

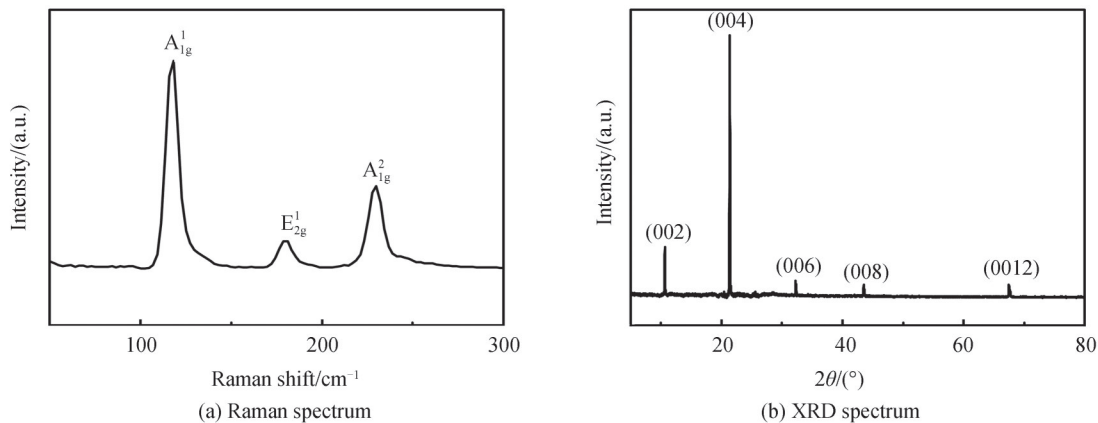


Fig. 1 The Raman and XRD spectrum of bulky  $\beta$ -InSe

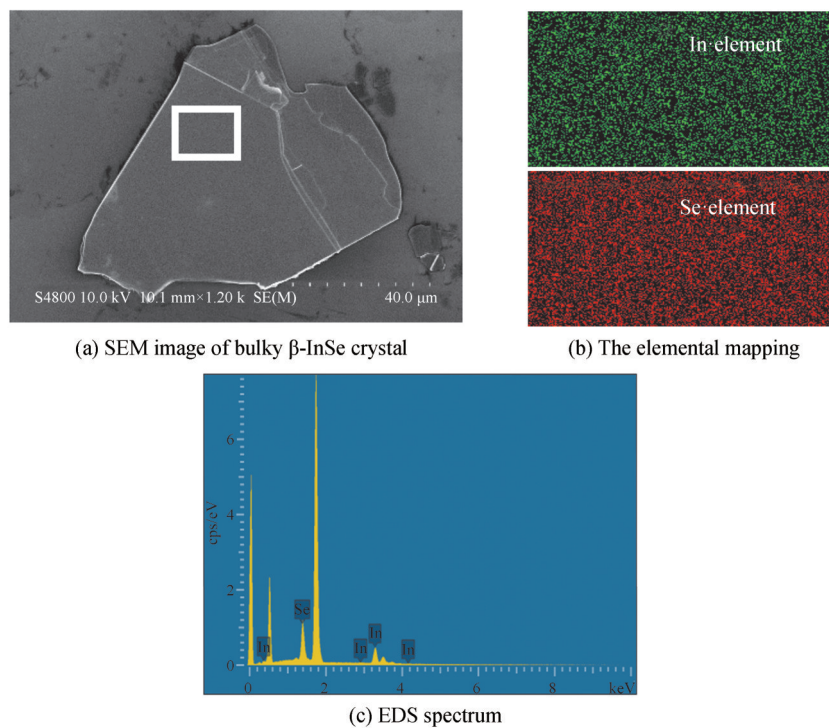


Fig. 2 The appearance and the composition of bulky  $\beta$ -InSe

We used the Liquid Phase Exfoliation (LPE) method<sup>[17]</sup> to fabricate the  $\beta$ -InSe SA. The  $\beta$ -InSe alcohol solution was prepared by mixing 1 mg  $\beta$ -InSe powder with 7 mL alcohol solution, then subjected to bath sonication for 3.5 h. Finally, we take the supernatant and drop it on the FC/APC fiber end face. The  $\beta$ -InSe will be transferred onto FC/APC fiber end face after the alcohol volatilized. The microscope image of the FC/APC fiber end face was shown in Fig. 3(a). It can be seen that the FC/APC fiber core was covered with  $\beta$ -InSe nanoflakes.

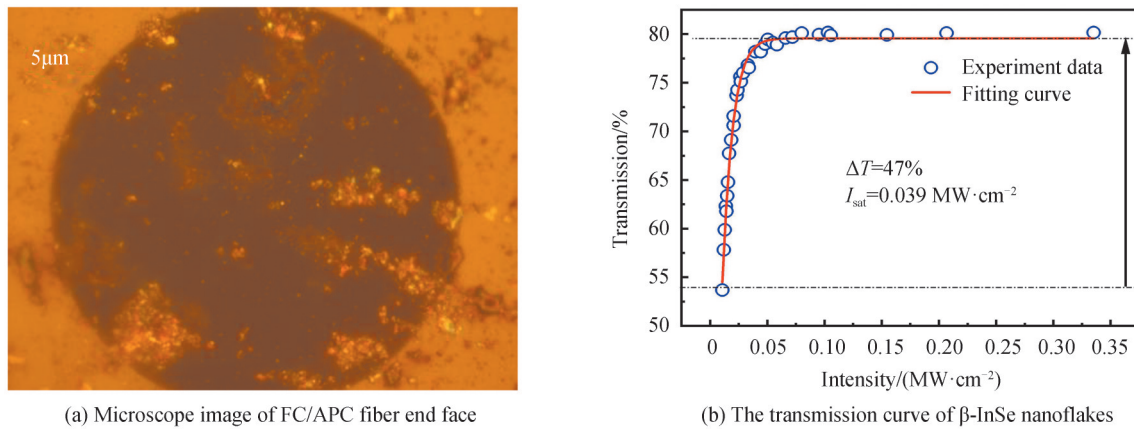


Fig. 3 The microscope image and the transmission curve of  $\beta$ -InSe SA

Used the twin-detector technique to investigate the nonlinear absorption properties of the  $\beta$ -InSe SA. A home-made Yb-doped Nonlinear Polarization Evolution (NPE) mode-locked fiber laser was used as seed source, which has a pulse duration of 120 fs, center wavelength of 1042 nm and repetition rate of 41.58 MHz. A Variable Optical Attenuator (VOA) was used for power regulation. The light splitted by a 50:50 fiber coupler, and one port passing through the SA was signal port and another was reference port. The transmittance curve of the SA as a function of pump power was demonstrated in Fig. 3(b). The saturable absorption mode was based on the following formula

$$T(I) = 1 - \Delta T \times \exp(-I/I_{\text{sat}}) - A_{\text{ns}}$$

where  $T$  is transmission,  $\Delta T$  is modulation depth,  $I$  is input intensity of the laser,  $I_{\text{sat}}$  is saturable power intensity and  $A_{\text{ns}}$  is non-saturable absorbance. By fitting the experimental results, the modulation depth and non-saturable absorbance in  $1 \mu\text{m}$  were 47% and 20%, respectively. The saturation intensity was  $0.039 \text{ MW}/\text{cm}^2$ .

## 2 Experiment setup and results

### 2.1 Q-switched Ytterbium-doped fiber laser

The experiment setup was shown in Fig. 4. A commercial 976 nm laser diode was used as pump source. The pump light was coupled by a 980/1030 wavelength division multiplexer. A 20 cm single-mode Ytterbium doped fiber (Liekki Yb 1200-4/125, Vancouver, USA) was used as gain medium, and Polarization Controller (PC) was used to adjust intracavity nonlinearity. The polarization independent isolator kept unidirectional operation in the cavity. A coupler (SR4889, AFR, Zhuhai, China) with 20% output was employed to output the laser. An 8 nm bandpass filter (BPF-1030, OF-Link, Suqian, China) was added to the cavity for wavelength selection. The total length of the cavity was 6.4 m.

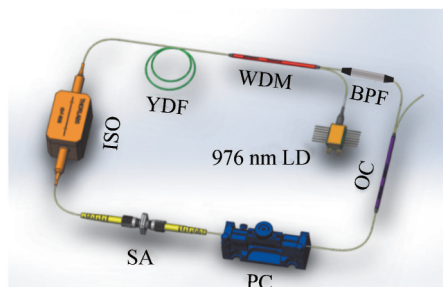


Fig. 4 Schematic of Yb-doped all-fiber laser

The laser characteristics were monitored by a real-time sampling oscilloscope (Tektronix DPO3052, 500 MHz, 2.5 GS/S, Shanghai, China) and an optical spectrum analyser (Ocean Optics HR2000, Shanghai, China) was utilized to record the optical spectrum. A photodetector (Thorlabs DET10A/M, Shanghai, China)

was employed to monitor the temporal evolution and output power of the output pulse train.

The Q-switched operation was realized by adjusting the PC and increasing pump power at 50 mW and the output power was 1.85 mW. The low Q-switching threshold benefited from the low saturation intensity and large modulation depth of SA. Besides, the low output power also indicated that there was a large loss in the cavity. The output power increased linearly with the increasing of pump power. With pump power increased to 350 mW, the maximum output power was 10.2 mW. However, when the pump power exceeded 350 mW, the Q-switched operation disappeared, because the SA was over bleached under the high pump power. As shown in the Fig. 5(a), with the pump from 50 to 350 mW, the repetition rate increasing from 53.42 to 217 kHz, while the single pulse duration decreasing from 1.7 to 0.63  $\mu$ s. As shown in Fig. 5(b), the maximum single pulse energy was 47.9 nJ. Figs. 5(c) and 5(d) illustrated the maximum 3-dB bandwidth of 3 nm and the minimum pulse duration of 630 ns at the pump power of 250 mW.

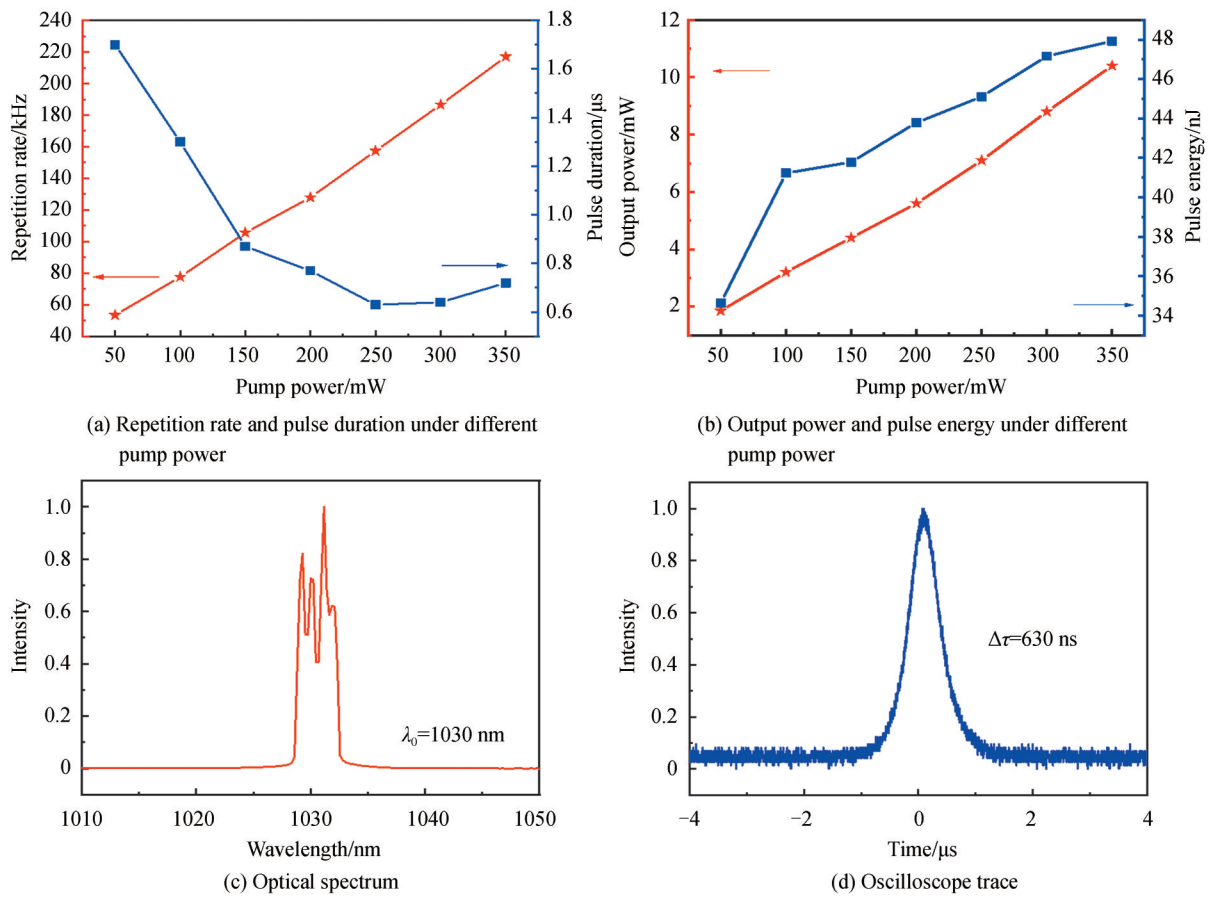


Fig. 5 The characteristics of Q-switched pulse in Yb-doped fiber laser

We compare with the passively Q-switched YDFL performance based on different 2D materials. As Table 1 shows, our work achieved the shortest pulse width of 0.63  $\mu$ s, highest pulse energy of 47.9 nJ.

**Table 1 Comparison of passively Q-switched YDFL performance based on different 2D materials**

SA	Q-Switched threshold/mW	Repetition rate/kHz	Min. pulse width/ $\mu$ s	Max. pulse energy/nJ	Wavelength/nm	Ref.
Fe <sub>3</sub> O <sub>4</sub>	80	25.9~73.4	3.4	38.8	1 049.8/1 053.3	[18]
MoS <sub>2</sub>	211.2	6.4~28.9	5.8	31.1	1 066.5	[19]
Bi <sub>2</sub> Te <sub>3</sub>	114	35~77	1	38.3	1 056	[20]
WTe <sub>2</sub>	110	19~79	1	28.3	1 044	[21]
Lu <sub>2</sub> O <sub>3</sub>	99	54.7~65.9	3.6	30	1 037	[22]
$\beta$ -InSe	50	53.42~217	0.63	47.9	1 030	This Work

## 2.2 Mode-locked Ytterbium-doped fiber laser

No mode-locking phenomenon was observed when we increasing the pump power or adjusting the PCs. The possible reason was that the cavity loss was too large to obtained the mode-locking operation. Therefore, we increased the YDF length to 40 cm. Then check the loss of devices in the cavity, and changed the FC/APC fiber connector.

We removed the bandpass filter because the actual spectrum was much smaller than the bandwidth of the BPF. In addition, the total cavity length was adjusted to 18.5 m, corresponding to a net dispersion of  $0.247 \text{ ps}^2$ .

When the pump power increased to 210 mW and carefully adjusted the PC, stable passive mode-locking operation was obtained. Under the maximum pump power of 700 mW, stable mode-locking operation can still be obtained by slightly adjusting the PC. As shown in Fig. 6(a), the output power increased linearly with the increasing of pump power. The maximum output power was 51.2 mW, corresponding to a single-pulse energy of 4.7 nJ. The output power against pump power showed a slope efficiency of 8%. The spectrum and oscilloscope trace at 700 mW pump power was shown in Fig. 6(b) and Fig. 6(c), respectively. the 3 dB bandwidth was 1.2 nm. and the repetition rate was 10.82 MHz corresponding to the cavity length of 18.5 m. It was worth noting that under the condition of high pump power. Obvious pulse splitting can be observed in the oscilloscope by adjusted the tightness of PC. As shown in Fig. 6(d), the repetition rate of 34.48 MHz was not an integral multiple of the fundamental frequency. Therefore we can eliminated the possibility of harmonic mode locking operation. The stable single pulse mode-locking operation can be achieved again by return the PC to its previous state. This phenomenon can be explained as follow: Pulse splitting usually occurred when the pump light was too strong or the single pulse energy was too large. Therefore, we can adjust the tightness of PC, which was equivalent to introducing some loss, to reduce the pulse energy and avoid the pulse splitting. However, the pulse duration of mode-locking pulse can not be obtained by using the autocorrelator (APE Pulse CheckUSB) in our laboratory, probably because the actual spectrum was relatively narrow. In addition, there was no dispersion compensation part in the cavity. A large number of positive chirps were accumulated in the

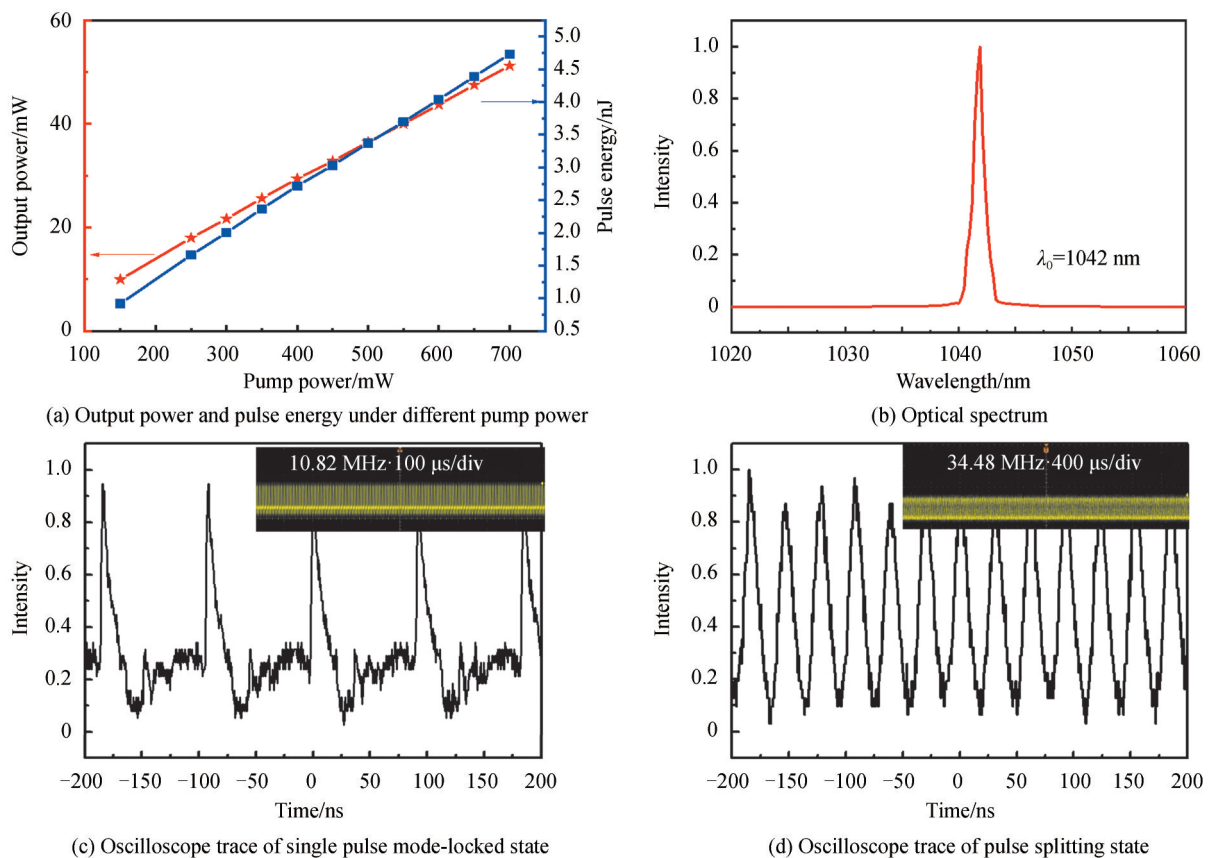


Fig. 6 The characteristics of Mode-locked pulse in Yb-doped fiber laser

cavity. Positive chirp would caused pulse broadening in time domain so that pulse duration of mode-locking pulse might exceeded the 50 ps maximum range of autocorrelator. Moreover, to further analyzed the stability of our YDFL system. We measured the function between time and the output power, which was shown in Fig. 7. The whole state was recorded for 24 h using a power meter. The calculated Root-Mean Square (RMS) is around 0.5% with mode-locked pump power of 550 mw and output power of 39.7 mW.

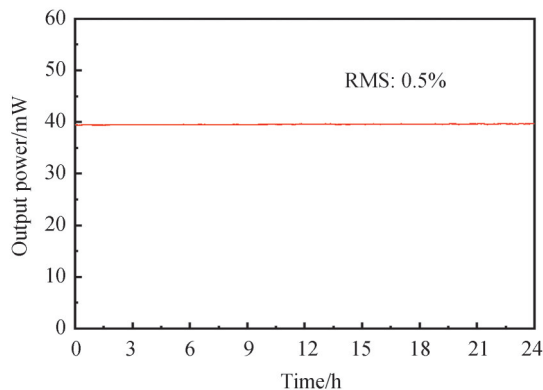


Fig. 7 The stability of mode-locked Yb-doped fiber laser

Table 2 shows the performance of previously reported passively mode-locked YDFLs based on different 2D materials as SAs. It can be clearly reflected that we obtained the highest output power of 51.2 mW, and highest pulse energy of ring laser cavity. Such laser with high output power is very promising for various applications such as fiber sensors, laser-machining, and many other industrial applications.

**Table 2 Comparison of passively mode-locked YDFL performance based on different 2D materials**

SA	Repetition rate/ MHz	Max. pulse Output power/ mW	Max. pulse energy/nJ	Wavelength/nm	Laser resonator	Ref.
Bi <sub>2</sub> Se <sub>3</sub>	44.6	33.7	0.756	1 031.7	Ring cavity	[23]
Sb <sub>2</sub> Te <sub>3</sub>	19.28	25.7	0.82	1 065.3	Ring cavity	[24]
MoS <sub>2</sub>	6.58	9.3	1.41	1 054.3	Ring cavity	[25]
WSe <sub>2</sub>	15.44	2	0.13	1 040	Ring cavity	[26]
SWCNT	27.3	3.47	0.13	1 030	Ring cavity	[27]
Bi <sub>2</sub> Se <sub>3</sub>	0.527	32.6	61.8	1 065	Linear cavity	[28]
$\beta$ -InSe	10.82	51.2	4.7	1 042	Ring cavity	This work

### 3 Conclusion

In summary, we report Q-switched and mode-locked Yb-doped fiber laser based on  $\beta$ -InSe SA for the first time. The maximum pulse energy of Q-switched pulse was 47.9 nJ and the minimum pulse duration was 630 ns. Stable mode-locking operation was successfully achieved with maximum output power of 51.2 mW, corresponding to a single-pulse energy of 4.7 nJ. The output power and pulse energy can be further improved by using a higher power pump source. Due to laboratory equipment limited, the pulse duration was not measured yet. It can be solved by introducing dispersion management element to compensate the positive chirp. This work proved the feasibility and application value of using  $\beta$ -InSe as saturable absorber in Ytterbium doped fiber laser. The saturable absorption characteristics and ultrafast nonlinear optical applications in other near infrared bands are also investigated in the future work.

#### References

- [1] KOESTER C J, SNITZER E. Amplification in a fiber laser[J]. Applied Optics, 1964, 10(3):1182-1186.
- [2] ZIRNGIBL M, STULZ L W, STONE J, et al. 1.2 ps pulses from passively mode-locked laser diode pumped Er-doped fiber ring laser[J]. Electronics Letters, 1991, 19(27):1734-1735.

- [3] WANG Jintao, CHEN Hao, JIANG Zike, et al. Mode-locked thulium-doped fiber laser with chemical vapor deposited molybdenum ditelluride[J]. *Optics Letters*, 2018, 43(9):1998-2001.
- [4] LIU Xiaojuan, HONG Zhifeng, LIU Ying, et al. Few-layer TaSe<sub>2</sub> as a saturable absorber for passively Q-switched erbium-doped fiber lasers[J]. *Optical Materials Express*, 2021, 11(2):385-397.
- [5] ZHANG Yue, ZHU Jianqi, LI Pingxue, et al. All-fiber Yb-doped fiber laser passively mode-locking by monolayer MoS<sub>2</sub> saturable absorber[J]. *Optics Communications*, 2018, 413:236-241.
- [6] LUO Zhichao, LIU Meng, GUO Zhinan, et al. Microfiber-based few-layer black phosphorus saturable absorber for ultrafast fiber laser[J]. *Optics Express*, 2015, 23(15):20030-20039.
- [7] GUO Zhinan, ZHANG Han, LU Shunbin, et al. From black phosphorus to phosphorene: basic solvent exfoliation, evolution of raman scattering, and applications to ultrafast photonics[J]. *Advanced Functional Materials*, 2016, 25(45):6996-7002.
- [8] DU J, ZHANG M, GUO Z, et al. Phosphorene quantum dot saturable absorbers for ultrafast fiber lasers[J]. *Scientific Reports*, 2017, 7:42357.
- [9] TAO Xin, GU Yi. Crystalline-crystalline phase transformation in two-dimensional In<sub>2</sub>Se<sub>3</sub> thin layers[J]. *Nano Letters*, 2013, 13(8):3501-3505.
- [10] CAI Hui, GU Yiyi, LIN Yuchuan, et al. Synthesis and emerging properties of 2D layered III-VI metal chalcogenides[J]. *Applied Physics Reviews*, 2019, 6(4):041312.
- [11] COSTA P G, DANDREA R, WALLIS R, et al. First-principles study of the electronic structure of  $\gamma$ -InSe and  $\beta$ -InSe[J]. *Physical Review B*, 1993, 48(19):14135-14141.
- [12] YAN Peiguang, JIANG Zike, CHEN Hao, et al.  $\alpha$ -In<sub>2</sub>Se<sub>3</sub> wideband optical modulator for pulsed fiber lasers[J]. *Optics Letters*, 2018, 43(18):4417-4420.
- [13] AHMAD H, ZULKIFLI A Z, YASIN M, et al. In<sub>2</sub>Se<sub>3</sub> saturable absorber for generating tunable Q-switched outputs from a bismuth-erbium doped fiber laser[J]. *Laser Physics Letters*, 2018, 15(11):115105.
- [14] HAI Ting, XIE Guoqiang, QIAO Zhen, et al. Indium selenide film: a promising saturable absorber in 3- to 4- $\mu$ m band for mid-infrared pulsed laser[J]. *Nanophotonics*, 2020, 9(7):2045-2052.
- [15] WANG Lizhen, LI Jianlin, CUI Yudong, et al. Graphene/ $\alpha$ -In<sub>2</sub>Se<sub>3</sub> heterostructure for ultrafast nonlinear optical applications[J]. *Optical Materials Express*, 2020, 10(11):2723-2729.
- [16] LI Lu, WANG Yao, JIN Wei, et al. Indium selenide saturable absorber for highenergy nanosecond Q-switched pulse generation[J]. *Applied Optics*, 2020, 60(2):427-432.
- [17] CUI Yudong, LIU Xueming. Graphene and nanotube mode-locked fiber laser emitting dissipative and conventional solitons[J]. *Optics Express*, 2013, 21(16):18969-18974.
- [18] AI-HAYALI S K M, AI-JANABI A H. Dual-wavelength passively Q-switched ytterbium-doped fiber laser using Fe<sub>3</sub>O<sub>4</sub>-nanoparticle saturable absorber and intracavity polarization[J]. *Laser Physics*, 2018, 28(3):035103.
- [19] LUO Zhengqian, HUANG Zizhong, ZHONG Min, et al. 1-, 1.5-, and 2- $\mu$ m fiber lasers Q-switched by a broadband few-layer MoS<sub>2</sub> saturable absorber[J]. *Journal of Lightwave Technology*, 2014, 32(24):4077-4084.
- [20] LEE J, KOO J, CHI C. All-fiberized, passively Q-switched 1.06  $\mu$ m laser using a bulk-structured Bi<sub>2</sub>Te<sub>3</sub> topological insulator[J]. *Journal of Optics*, 2014, 16(8):085203.
- [21] KO Seunghwan, LEE Jinho, LEE Juhan. Passively Q-switched ytterbium-doped fiber laser using the evanescent field interaction with bulk-like WTe<sub>2</sub> particles[J]. *Chinese Optics Letters*, 2018, 16(2):020017.
- [22] JAFRY A A A, KASIM H, ROSOL A H A, et al. Q-switched ytterbium-doped fiber laser based on evanescent field interaction with lutetium oxide[J]. *Applied Optics*, 2019, 35(10):9670-9676.
- [23] DOU Zhiyuan, SONG Yanrong, TIAN Jinrong, et al. Mode-locked ytterbium-doped fiber laser based on topological insulator: Bi<sub>2</sub>Se<sub>3</sub>[J]. *Optics Express*, 2014, 22(20):24055-24061.
- [24] KOWALCZYK M, BOGUSLAWSKI J, ZYBALA R, et al. Sb<sub>2</sub>Te<sub>3</sub>-deposited D-shaped fiber as a saturable absorber for mode-locked Yb-doped fiber lasers[J]. *Optical Materials Express*, 2016, 6(7):2273-2282.
- [25] ZHANG H, ZWENG J, DU J, et al. Molybdenum disulfide (MoS<sub>2</sub>) as a broadband saturable absorber for ultra-fast photonics[J]. *Optical Express*, 2014, 22(6):7249-7260.
- [26] SAMIKANNU S, SIVARAJ S. Dissipative soliton generation in an all-normal dispersion ytterbium-doped fiber laser using few-layer molybdenum diselenide as a saturable absorber[J]. *Optical Engineering*, 2016, 55(8):081311.
- [27] GUO Hongyu, HOU Lei, WANG Yonggang, et al. Tunable ytterbium-doped mode-locked fiber laser based on single-walled carbon nanotubes[J]. *Journal of Lightwave Technology*, 2019, 37(10):2370-2374.
- [28] HAN Xile, ZHANG Huanian, ZHANG Chao, et al. Large-energy mode-locked ytterbium-doped linear-cavity fiber laser based on chemical vapor deposition-Bi<sub>2</sub>Se<sub>3</sub> as a saturable absorber[J]. *Applied Optics*, 2019, 58(10):2695-2701.